

DYNAMIC WETTING OF WATER AND OIL ON NANO AND MICROSTRUCTURED SURFACES ON PLANTS

Abstract

For more than 460 million years, the various structures on the surface of plants have encouraged many practical structures that have been highly adapted. Structural and chemical changes are made in the plant cuticle for surface moistening which range from superhydrophilic up to superhydrophobic. In this review, we documented the nano and microstructure molecule which were the responsible the wetting of oil and water on leaf surface of the plants. Plants wetting is affected by the cell sculptures and fine surface structure, such as cuticle folding, or epicuticular waxes. Hierarchical structures are seen on plant surfaces and more forms of plant surface structures are introduced to superhydrophobicity and superhydrophilicity. The surface of superhydrophobic and superhydrophilic have several applications such as liquid transport in capillary, drift reduction for water transport and self-cleaning.

Keywords: direct laser interference patterning, nanosecond and picosecond laser pulses, multi-scale microstructures, wettability transition

1. Introduction

The surface of biological have deliver a wide range of structures and abilities, for example self-healing and self-assembly. Their properties and structural variety evolved over numerous millions of years through a long lasting game of selection and mutation. Adaptation results with diverse conditions and the wider system versatile, protects the growth of the interface.¹⁻² They are suitable for a extensive range of the biologically inspired materials of the artificial. The prominent cases are water repulsive and self-cleaning fabrics, which are based on surface characteristics and are created using a biological model of lotus leaves and surfaces that minimize drag while passing through the water, such as the skin of the hips.³⁻⁵ The various structures of the surface plant depends on the variable cell shape, micro and nano-structures on the cell surfaces and on the creation of multicellular.¹ The greater structural complexity and functional surfaces on plants are focused on these cellular and sub-cellular units, an almost infinite mix of structures.⁶ Surface properties of plants include mechanical stability, the availability of an effective barrier to water transpiration and the removal from the inside of living cells of the molecules.⁷⁻¹⁰ Plant surfaces' structural properties include development of low-adhesive surfaces, such as insect slides, and an improvement in visible light reflection or in the absorption of dangerous UV radiation.¹¹⁻¹⁴ Plant surface structures are

also important for the weight resistance of the soil. Superhydrophilosity means an immediate distribution of a droplet placed on a surface that does not even calculate the contact angle.¹⁵ On the other side, water remaining in a superhydrophobic surface as a small globular droplet with a contact angle approaching 150°.¹⁻² Surface wetting is connected to the structuring of surfaces and to surface chemistry; these are thus briefly mentioned in the following.¹ The epidermal cells cover all principal surfaces of plant, such as petals; leaves; fruits; and herbaceous stems, as the outermost cell layer.¹ **Figure 1** depicts a simplified epidermal cell layer.

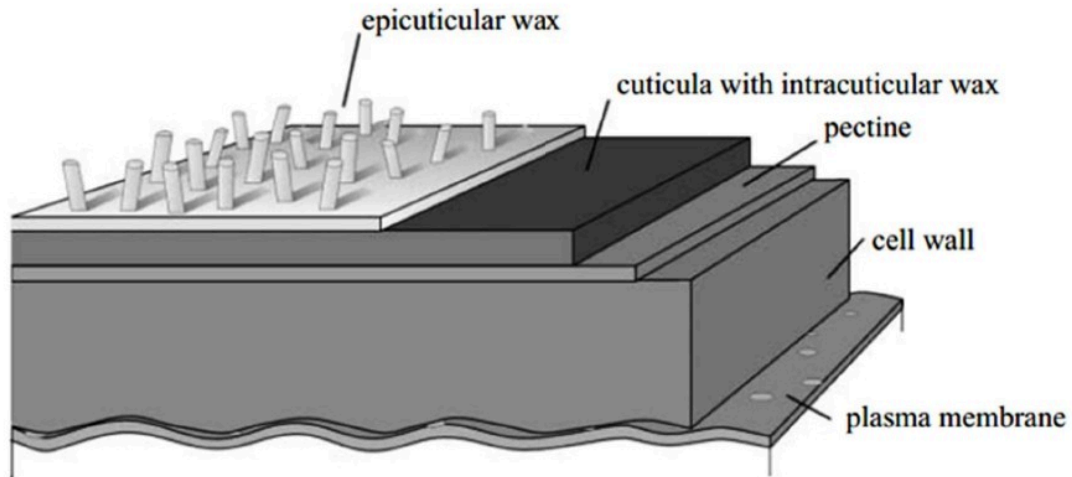


Figure 1: simplified epidermal cell layer

The role as a transpiration obstacle is one of the most significant qualities of the cuticle.¹⁶ The cuticle consists essentially of a cutin polyester, with built-in and superimposed waxes.¹⁷ The network of cuticles is made of cutin and even cutanes or other polymers known as lignin occasionally.¹⁸⁻²¹ A pectin layer is shown in Figure 1. The plasma membrane is the last layer seen, which separates from the external, non-living epidermis the alive cell compartment with the containing of water cell.

1.1 Micro and nanostructures of plant surfaces

1.1.2 The microstructures of plant surfaces

A single epidermal cell is a plain unit for the surface structuring. Plant surfaces micromorphology is created by an epidermal cell's outline and sculpture. The primary sculpture includes the outline of the anticlinal two walls and the curvature of the external periclinal cell wall (outer portion cell). The curve of cell is tabular (flat); convex (outward) and concave (inward) where the most common cell shapes is the convex. The cell form is also convex.

Convex cells can be divided into different subtypes, such as hemisphere, cupola, tube, papilla, hair papilla, and the hair according to their form and aspect ratio (height to width ratio) (Koch et al. 2008a). Hair or trichomes are classified as epidermal cells that have a 7:1 or higher aspect ratio. Wagner has studied the nature of hair morphology and its roles.²²⁻²³ Hair may also consist of many cells (multicellular hair) in plants and examples will be later added and their value for surface wetting.

1.1.3 The structures of cell surfaces

There are two types of structuring of the cell surface in plants: one is epicuticular waxes and another is cuticular patterns. For a number of biogenic products the word “wax” is used in different kinds of fatty materials.²⁴⁻²⁵ Bees wax, paraffin and carnauba wax are well-known examples. Hydrocarbons of aliphatic and derivatives are the main components of plant waxes. Lengths of carbon chain were varying from 20 to 40, and approximately 60 atoms for esters (two linked chains). There are many researcher work on the chemical components of plant waxes.²⁶⁻²⁸ Waxes of plants have a highly variable chemical composition in plants or organs and also during organ growth (for example, upper or lower sides of the leaves).²⁹ The compositions are primary or secondary ketones, alcohols, aldehydes and fatty acids. In plants waxes, alkanes are found in low concentration. Many compounds are present more seldom in plant waxes but may be the dominant compound in those waxes where they occur. The Primary alcohols and aldehydes were the major wax of *Hedera helix*.²⁴⁻²⁵ Fatty acids C24–C30 and primary alcohols C24–C2 were the main compounds of *Magnolia grandiflora*. Alkanes C29, C31 are present in *Prunus laurocerasus*. *Crassula ovate* have present Aldehydes C30, C32, alkane C31. Beta-diketones C33 is the major compound of *Eucalyptus globulus*. Beta-diketone C31 and hydroxy-beta-diketone C31 are the present in *Leymus arenarius*. Secondary alcohol C29 and secondary alkanediols C29 are present in *Ginkgo biloba* and *Nelumbo nucifera* respectively. Secondary alcohol C29 is present in *Thalictrum flavum glaucum*, *Tropaeolum majus* and *Tulipa gesneriana*. Primary alcohol C26, C28 and aldehydes are present in *Convallaria majalis*.² Primary alcohol C26² and aldehydes² are present in *Euphorbia myrsinites*.² Primary alcohol C26 is the composition of *Galanthus nivalis* and *Iris germanica*. Primary alcohol C28 is the component of *Triticum aestivum*. Ketones are the components of *Aristolochia tomentosa* and *Liriodendron chinense* respectively. Alkanes C31 and Triterpenol acetates are the composition of *Gypsophila acutifolia* and *Benincasa hispida*. Almost all of the data on the chemical components of plant waxes is based on waxes derived from solvents.² There are epicuticular and intracuticular wax mixtures, which can vary chemically.³⁰⁻³¹

Epicuticular waxes are crystalline and take place in various morphologies of 0.2 to 100 nm in size.³²⁻³⁶ The morphologies of some common wax are transversely ridged rodlets (*Sassafras albidum*); films (*Hydrocotyle*); platelets (*Robinia pseudoacacia*); crusts (*Crassula ovata*); rodlets (*Brassica oleracea*); β -diketone tubules (*Eucalyptus gunnii*); and nonacosan-ol (*Thalictrum flavum glaucum*). The composite structure for the 3D-wax film is not demonstrated with the scanning electron microscopy (SEM). Thus, the waxes of epicuticular have been transferred to a smooth artificial surface using a simple method of mechanical isolation.

The experiments of recrystallization with isolated waxes have shown that the various morphologies of wax emerge from self-assembly.³⁷⁻³⁸ They reported the identical morphology of the waxes recrystallization on the plants of surface. The atomic force microscopy (AFM) was used as the study in self assembly method.³⁹ AFM have effective solving power to work with live plant material for image nanostructures with Normal Temperature and Pressure (STP).

The structure of the 2nd type of the cell surface is derived from the cuticle structure. Almost all surfaces of the ground plants have identified such type patterns of cuticle, but they are most often found in the flowers (petals) and seed surfaces. They follow the patterns as folding or as tubercular (verrucate) that emerge from the cuticle itself.⁴⁰

1.3 Classification of wetting surface

Wetting is the main fluid interaction mechanism on solid-gas interfaces. It defines the interaction of a liquid with a solid surface. Here we documented some of basic concept of surface wetting. Relevant books, including the books of Israelachvili (1992); De Gennes et al. (2004) and Bhushan (2008); are recommended for a more thorough review. The wetting of the surface is classified by two ways, one is Wenzel and another is Cassie-Baxter.

Wenzel first described the idea of wetting a rough surface.⁴¹ He said that if a liquid wets away a solid surface favourably with the thermodynamic claim on the raw surface, wettability is increased.² Similarly, the resistance to wetting of the surface increases when the surface is rough. The Wenzel equation gives the apparent angle of contact on a totally wet, rough surface. The equation is shown in Eq 1.

$$\cos \theta_w = r \cdot \cos \theta \quad (1)$$

Liquid absolutely wets each area on the coarse surface in the state of Wenzel.⁴¹ The roughness improves wettability and hydrophilic material is converted to superhydrophilic.⁴¹⁻⁴² The resistance of the surfaces to wet for moderately hydrophilic and hydrophobic material is

improved by roughness.^{2,41-42} The advancing contact line often prematurely pins the liquid droplet into an abnormally wide contact angle.^{2,41-42} The vibration of the drop de-pins the line and shift it to a balanced position, the contact angle being a smaller equilibrium.^{2,41-42} The measured angle of the Wenzel is consistent with confirming the vibration contributes to the rough surface's most stable wetting phase.² Roughness geometry has a profound influence on the wetting and propagation process.² While cavities and pores wet the surface similarly to the smooth surface, bumps interfere with the contact line on the other side; it delays the advancement of the contact line during spreading and the recession of the contact line.^{2,41-42} In the Cassie Baxter state, bags of air during liquid wetting are trapped and established the composite interface of liquid-solid-air.^{2,41-42} This interface features a broad interface with slight sliding angle and contract angle.² The surface of low energy material, texture or roughness surface and re-entrant geometry are key strategy factors for both superoleophobicity and superhydrophobicity.^{2,41-42} Since the Wenzel state is typically more stable, a lot of consideration has been paid to stabilizing the state of Cassie-Baxter, by increasing their energy barrier.^{2,41-42} The hierarchical re-entering and roughness angle in the liquid-solid-air interface are proof of being necessary for not only stabilizing the composite state of Cassie-Baxter to Wenzel but also, in applying external pressure, to increase its collapse resistance.^{2,41-42} Composite of Cassie-Baxter state on the groove surfaces, leading to directional wetting, may also be created.^{2,41-42} Droplets are seen to move faster in the parallel direction with the grooves when the firm strips are wetted. The developing contact line is obvious by imagining the hot polyethylene wax. The contact line moves in the orthogonal direction from the one solid to another strip. This increases pinning likelihood and leads to a wide contact angle and a sliding angle.^{2,41-42} Surface with interesting unidirectional distribution has been reported with acceptable surface texture.^{2,41-42} Despite its fascinating wetting characteristics and various potential applications, rough surfaces are delayed with technology implementation.^{2,41-42} The main challenge is addressed to cross the gulf between research and product.^{2,41-42}

1.3.1 Wenzel

From Wenzel equation (1), hydrophilate rough surface with a very small contact angle $\theta < 10^0$ can become superhydrophilic.⁴¹ The rough surfaces, however, can result in areas with high contact angles with moderately hydrophilic and hydrophobial materials.⁴¹ In general, the wetting process is energetically beneficial when a surface is totally wetting by liquid.⁴¹⁻⁴²

(a) Most stable and metastable Wetting State

The manufacture of four rough surfaces by coating beeswax with a glass slid and three bristle papers (attached to glass slides), with a roughness range of Wenzel r 1.03-1.25, as determined by the abrasive paper grit number, is reported by Meiron, Marmur and Saguy in 2004.^{2,43} The energy on the surface of these surfaces should be very similar since they have been made from the same wax.⁴¹ Before and after vibration through a loudspeaker, the contact angles of water and ethylene glycol were studied on these four surfaces.² The f_A demonstrates the speed of the loudspeaker vibration movement.

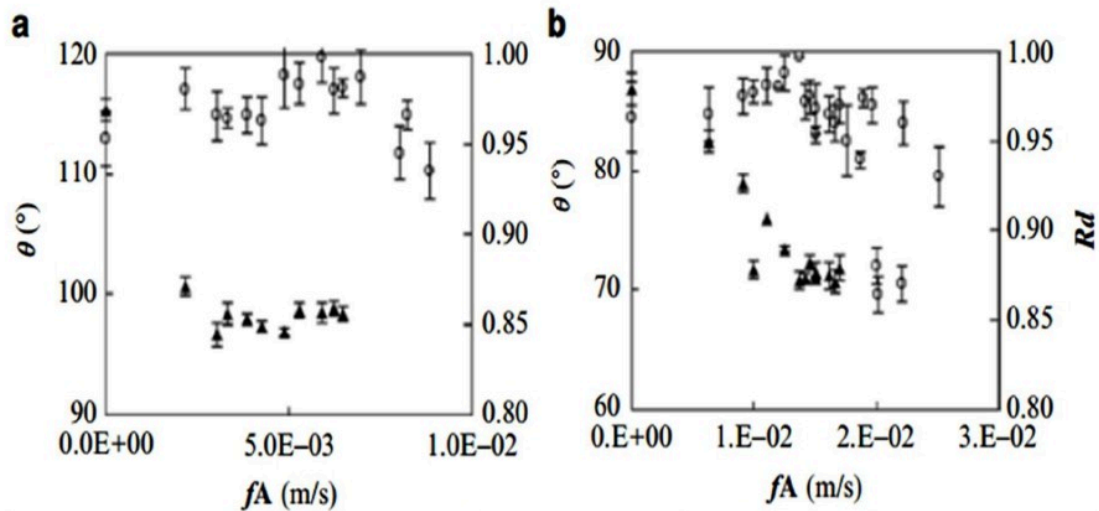


Figure 2: θ (contract angle) vs R_d (drop roundness) is a work the function of speed f_A on the surface with $r = 1.09$ (a) water and (b) ethylene glycol.^{2,43}

Figure 2 is used from the research paper of Meiron, et.al.⁴³ In Figure 2, the surfaces with $r = 1.09$ shows plots of the effect of f_A on contact angle and roundness (R_d) of the water and ethylene glycol droplets.² Drops of $R_d > 0.95$ are usually considered.²

The results show clearly that the droplets are vibrant with the speaker, de-pins contact lines and allows objective with smaller contact angles into a more secure wetting state.^{2,41} The contact angles of the Wenzel (θ_w) for water and ethylene glycol were shown to decrease at $\sim 115^\circ$ and $\sim 85^\circ$, respectively, after vibration at $\sim 98^\circ$ and $\sim 71^\circ$ subsequently. The results show that both water and ethylene glycol have metastable in initial droplets. Reasonable vibration contributes to metastable weighing states with balance angles at θ_w^{eq} in their most stable wetting conditions.⁴¹

The data in **Figure 2** actually support this free energy relationship. For example, the viscosity of ethylene glycol is higher than that of water.² The energy barrier for the advancement of fluid is higher on the same rough surface for ethylene glycol.² Indeed, the analysis of the f_A values in **Figure 2** shows that the ethylene glycol droplet requires approximately 10 times more energy compared with water to equilibrium.² θ_w^{eq} values of rough surface on ethylene glycol and water is calculated from equation Eq. (1) through using Wenzel angle $(\theta_w)^{cal}$.² There is a very strong consensus. The agreement promises that the apparent contact angle θ_w on rough surfaces is metastable, as is the case with a smooth surface. As all its kinetic energy is dissipated by friction from the rough surface, liquid droplet only ceases to spread.² This contributes to a value of θ_w greater than expected. When a vibration noise excites the metastable wetting status, the contact line de-pins and proceeds to move to the most stable wetting status at an equilibrium angle of θ_w^{eq} .²

(b) Unpredicted Wettability

The Wenzel equation indicates that the wet of the hydrophilic surface should be increased by roughness.² This especially refers to very hydrophilic materials (water $\theta < 30^\circ$), which have sometimes contributed to super-wetting or superhydrophilicization.⁴⁴ On the other side, it was not well studied to wet on rough surface of moderately hydrophilic material. A research on wetting the microtextured surfaces of square pillars made up of SU8 was carried out by Forsberg and co-workers in 2010.⁴⁵ SU8 is widely used photolithographic material and with water $\sim 72^\circ$, it is slightly hydrophilic. The pillar width is set at $w=20 \mu\text{m}$;² the spacing d is 25 to $120 \mu\text{m}$, and the sample height is 7 and $30 \mu\text{m}$.² The surfaces show a receding angle of almost 0° and an image of the meniscus is reflected on the insert after the water receding. This indicates that the surface of the SU8 pillar is entirely driven by water. The hydrophobic pillar arrangement surface was carried out in additional control experiment. With a large fixed contact angle small hysteresis was obtained, providing that droplets of water were indeed present Cassie - Baxter the state of the box on the surface of the hydrophobicized pillar array.² With the total wetting data, one can determine that the SU8 Pillar array surface water droplet is in the Wenzel condition.⁴¹

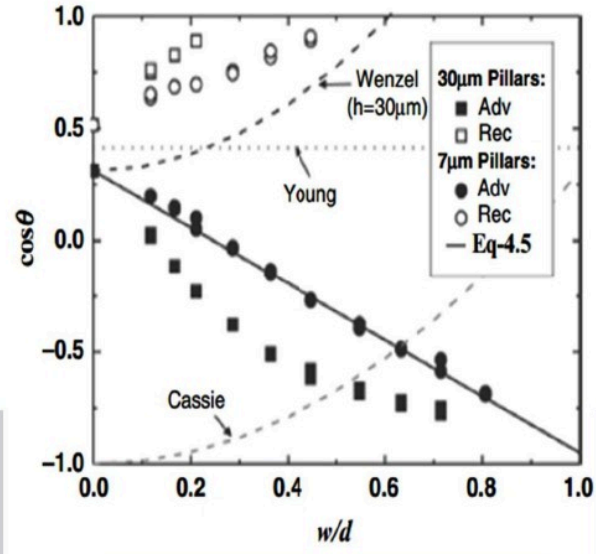


Figure 3: Plot of $\cos\theta$ vs w/d for SU8 square pillar array surfaces.^{2,45}

The advancing and withdrawing contact angles of the SU8 pillar array surfaces in function of w/d are shown in **Figure 3**.^{2,45} The top line of the dash indicates the pattern from the equation 1 of Wenzel.² There is no difference between the observed advancing contact angles and the measured data; they move in an opposite direction.² Forsbery et.al believed that the Liquid – Solid-Air interface had a mechanical-stable configuration to explain the unexplained broad contact angle and the discrepancy between the Wenzel equation and experimental results.² Then they used the geometry and dimension of the contact line to adjust the ruggedness factor of Wenzel.² The modified equation of Wenzel is given by:²

$$\cos \theta_w^{\text{mod}} = \left(1 - \frac{w}{d}\right) \cdot \cos \theta_{\text{SUS}} + \left(\frac{w}{d}\right) \cdot \cos \left(\theta_{\text{SUS}} + \frac{\pi}{2}\right) \quad (2)$$

The solid line was calculated from $\cos \theta_w^{\text{mod}}$ shown in Figure 3. The modified angle of the Wenzel and the angle observed for the pillar array surfaces are achieved with a height of 7 μm pillars.² The observed apparent contact angles were also greater in the pillar range surfaces with 30 μm pillar height.⁴¹ The variance with the measured values of equation 2 is due to the fact that the updated equation uses a low pillar height. In either case, this research confirms the principle that the contact angle is determined by the point of contact, not the region of contact below the fluid droplet.⁴¹

(c) Dynamics Wetting and Wettability of Roughness Geometry

Kanungo and co-workers were recently produced with the use of conventional photolithography and moulding techniques a series of model rough PDMS surfaces including a range of the 3 μm hemispherical bumps, and pitch cavities of between 4.5 and 96 μm .² Kanungo and co-workers were recently produced with the use of conventional photolithography and moulding techniques a series of model rough PDMS surfaces including a range of the 3 μm hemispherical bumps, and pitch cavities of between 4.5 and 96 μm .^{2,46} **Figure 4** shows the representative SEM micrographs.

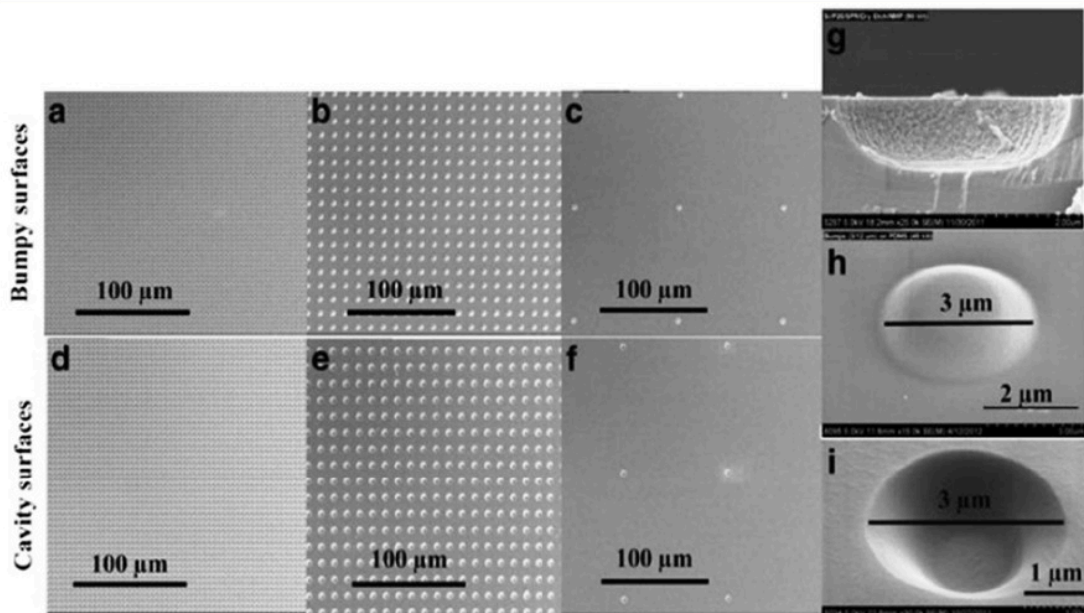


Figure 4: SEM of PDMS with varying pitches (a, d 4.5 μm ; b, e 12 μm and c, f 96 μm); (g) hemispherical silicon mold 3 μm diameter, (h) hemispherical bump on the PDMS surface created from the mold in (g) and hemispherical cavity PDMS surface molded from the bumpy surface in (g).^{2, 46}

Figure 4 shows a rather comparable, significantly smaller than 90° , wetting angle between real, coarse surfaces and the bumpy and crack surfaces.² While the majority of the model rough surfaces in the literature are high aspect ratios pillar arrays.^{2,45,47-49} Pillars are vertical fluid protrusions and the wetting angle in the incoming liquid toward the advancing fluid is 90° .² Friction of the pillars applied to the advancing liquid is supposed to be greater than those from hills and valleys and even from bumps and cavity surfaces based on basic geometrical

consideration.² Other work objectives included studying the impact of rough geometry on surface wettability and dynamics of wetting, using bumps and cavities as models for hills and valleys.^{2,41}

(d) Practical Consequences

The ability to moisturise each cavity or hole on a rough surface benefits both from nature and the use of human resources. Water spreads without trap air and without a measured contact angle spontaneously when a super hydrophilic surface wets. In nature, these surface structures have been produced in plant leaves to adapt plants to their living environment and to survive.⁵⁰⁻⁵¹

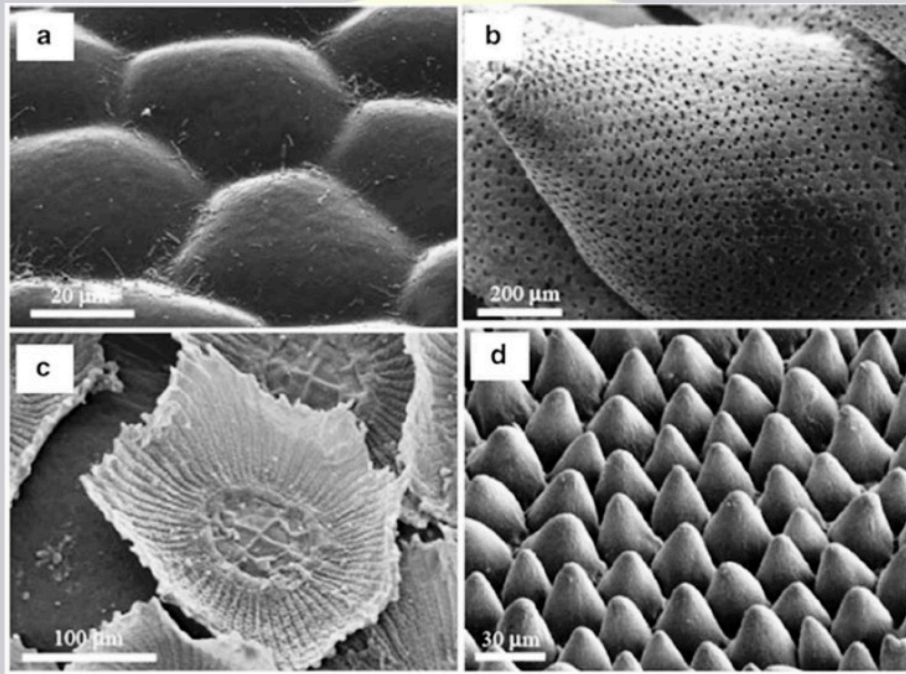


Figure 5: SEM of superhydrophilic plant leaves (a) *Anubias barteri*, (b) *Sphagnum squarrosum*, (c) Spanish moss *Tillandsia usneoides*, and (d) *Calathea zebrina*.^{2, 50-51}

For example, in submergent plant leaves of water the microstructures are smooth, allowing water to wet the surface uniformly while preventing fouling (**Figure 5a**). Conversely, the microstructures of aquatic plants are structurally more complex, such as different mosses (**Figure 5b, c**). These leaves are intended for water and nutrient uptake and are designed to hold the water onto a superhydrophilic surface with a structure. Plant leaves from *Calathea zebrina*

(Figure 5d) are to be found a very simple micro-structure because it has only to spread water on the surface very fast.

Many superhydrophilic artificial surfaces are recognised and the TiO₂ film is the most prominent.⁵² The surface shall be prepared with a precursor sol-gel on a substrate and then the coated surface shall be scrubbed into a furnace.² The film of TiO₂ is mildly hydrophilic essentially.² Its superhydrophilicity is activated with radiation from UV or sunlight.² Similar to TiO₂, hydrophilic particles are often silica and other metal oxide. Thin films may be applied by solar gel or deposition by sheet, or as a plastic coating using a polymer binder.^{2,53-55} Finally, a completely wetted liquid-solid interface should also be beneficial to heat exchange equipment and electrodes, which can minimise overheating and over-potential.²

1.3.2 Cassie-Baxter

Effect on Lotus

When a fluid is on the rough surface, the droplet is normally in the condition of “Cassie Baxter”, a wide contact angle with a small angle of sliding is characterized.² For water, a superhydrophobic surface is named. The Lotus Leaf, which shows 162 ° contact angle of water and a 4° sliding angle, is the most prominent superhydrophobic surface.⁵⁶ When rolling off, particles of dirt and dust cling to the water droplet, which contributes to the so-called self cleaning effect.² These statements has encouraged many worldwide researchers and superhydrophobicity lessons have evolved meanwhile.²

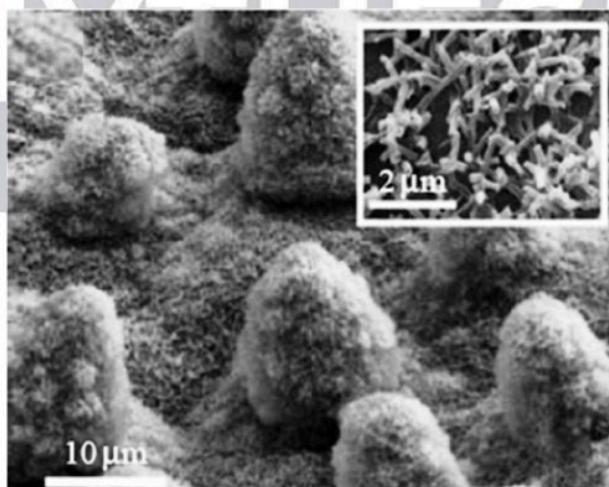


Figure 6: SEM of the surface of Lotus leaf⁵¹

Figure 6 depicts SEM morphology on the surface of the leaf, which include micron aggregated wax crystals allotted randomly over 10–20 μm of papillae and carpeted with a layer of waxy nanohairs over the entire leaf surface.^{50-51,57-59}

Superhydrophobic Artificial Surfaces

The research activities on superhydrophobicity is exponentially increased from inspired by the Lotus effect.⁶⁰⁻⁶¹ A water contact angle of > 150 degrees and the slider angle of 10 degrees or less shall have the consensus explanation for a superhydrophobic surface.⁴² This definition is rather arbitrary and has now been published with a more refined definition.⁶² Superhydrophobic surfaces and self cleaning influence have been used in many potential applications, like, microfluidic devices, windows of self-cleaning, transportation, textiles, fuel, clothing of soil-resistant, gas, display and surface of i-phone, drag reduction in ship, coating of anti icing, structures of metal, roof top of airplane and coatings of corrosion-resistant for bridges.² Many surfaces / coatings have to date been documented in artificial superhydrophobia and the topic has also been reviewed in recent literature.⁶³⁻⁶⁸

The key parameters dependent on Wenzel and Cassie-Baxter's work, Roughness and hydrophobic surface cover are superhydrophobic.⁴¹⁻⁴⁴ Top down / bottom up methods or moulding and, embossing may be used to produce roughness.² The literature has examined detailed explanations of these processes and won't be comprehensive here. The roughness in the top-down approach results in a smooth surface with a power beam or an etching agent or, if the material itself is not hydrophobic, changes the surface with a hydrophobic coating. Significant efforts have been made on the surface of the pillar array where Cassie-Baxter-to-Wenzel transformation has been investigating the properties of surface chemistry and roughness on the contact angle, hysteresis and weaving stability.^{2,69-72} The coarseness and solid-area fraction of the pillar picture surface are regulated by pillar size and geometry, length and the height of the pillar.⁴¹ These surfaces are normally made by a lithographic or e-beam grafting technique followed by surface hydrophobisation with an the alkylsilane / perfluoroalkylsilane.² The preparation of the $5 \times 5 \mu\text{m}$ tetragonal pillar (height = $5 \mu\text{m}$) surfaces of variable pitches was recorded by Byun and his coworkers in order to model the wettability of insect wings.^{2,72} Photolithographs on the silicon wafer arranged as the model surfaces. The final texture was changed with a fluorosilane FOTS layer on the surface.² The fluorinate self-assembled-monolayer was manufactured by using 'tridecafluoro-1,1,2,2-tetrahydrooctyltrichlorosilane'.²

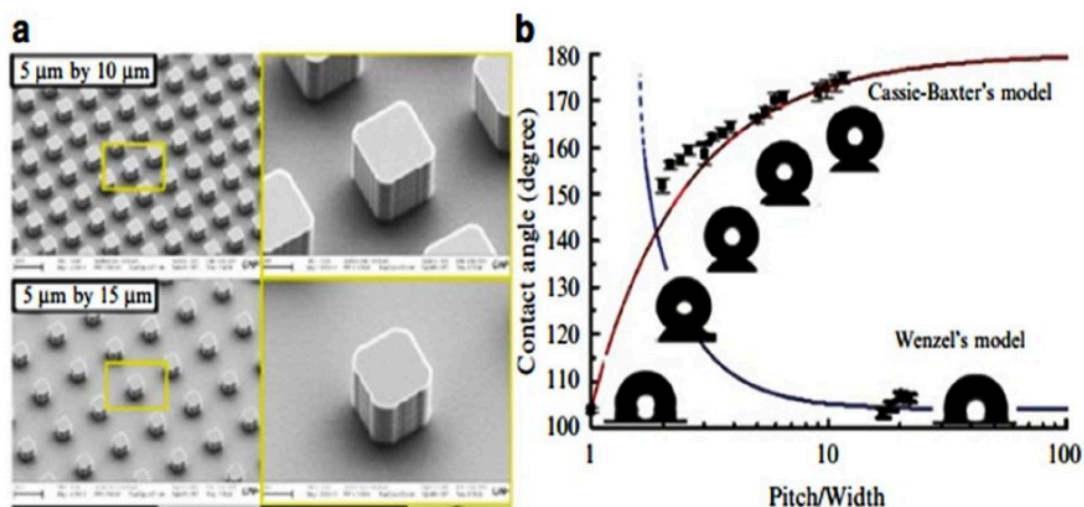


Figure 7: Pillar array FOTS surface (a) SEM of and (b) contact angle vs pitch/width⁷²

Figure 7a represents the SEM morphology of pillar array FOTS surface. In plot of the pitch / width ratio, the water angle of contact for the model surface are indicated (**Figure 7b**).⁴¹ The results demonstrate that the contact angle initially increases with a pitch / width ratio. The pitch / width ratio of 2 to 15 indicates that these surfaces are superhydrophobic with high contact angles that are expected by the model of Cassie-Baxter.² At pitch / width as ≈ 15 , a transition occurs. The value of pitch/width is more than 20 suggested that sloping aquatic interface affects the lowermost of the surface array of pillar.² As a consequence, the whole surface is completely wetting.²

Transition to Wenzel State from Cassie–Baxter

It has historically been recognised that micro-/nano-rough surfaces can be present, depending on the experimental conditions, in both Cassie-Baxter and Wenzel wetting states. He et.al and his co-worker have shown that water droplets on a PDMS microtextured surface are in Cassie – Baxter state if they are gently dispensed.⁷³ In comparison, when the drop is dispensed, a Wenzel droplet is attained in some height. The results show that the droplet of Wenzel is the more stable. Quere et al formed a Cassie-Baxter droplet with θ_A of 163° surface on a fluorinated microtexture in an experiment that was somewhat different.⁷⁴⁻⁷⁵ If an external pressure is applied, this droplet from Cassie can be transformed to a Wenzel droplet. On the same surface, the condensation experiment could also produce a similar Wenzel droplet. Bormashenko and the team demonstrated that the droplet Cassie could be removed and formed the droplet of Wenzel through vibration noise.⁷⁶⁻⁷⁷ Boreyko and Chen have shown that condensing water on a high humidity Lotus leaf will vibrate the droplet from the Wenzel to the Cassie droplet. Liu and colleagues who were able to transform a droplet from Wenzel into the droplet of Cassie by

heating are another example of the exciting Wenzel droplet.⁷⁸ Although the state of Wenzel is stable, the overall findings seem to show that, depending on the experimental situation, they are interconvertible. The experimental condition means that (1) there is a barrier of energy between them and (2) they may have a small difference in energy.

Surfaces with high water repellence and self-cleaning are required in most practical applications. Approaches to boost Cassie-Baxter's stability include increasing or better stabilisation of the energy barrier among these states and making Cassie-Baxter more stable. Theoretical analytical and experimental results show that the energy barrier between Cassie-Baxter and Wenzel would be increased by a Hierarchical, multi-size ruggedness structure, a re-entrant and hydrophobic surface coating.⁷⁹⁻⁸³ The barrier height rise not only increases the metastable stability of the Cassie-Baxter, its resistance to external pressure will also be improved. In addition, there is a provision for the thermodynamic advantage of the state of Cassie-Baxter under certain structures of hierarchical roughness.⁸²⁻⁸³

Superoleophobicity

Hydrocarbon oil has much lower surface tension than water. Hexadecane was used regularly as an oleophobic sample liquid and its surface tension was nearly three times lower than that of water (27.5 vs. 72.3 mN / m). As a consequence, it wets most surfaces. The smooth surface of the hexadecane $\theta > 90^\circ$ is even more difficult. Super hexadecane repellence surface is therefore unusual. Surface area with hexadecane contact angle $> 150^\circ$ and sliding angle $\sim 10^\circ$ is the representation of the overall superoleophobicity. In comparison to super-hydrophobic, superoleophilic surface, it is anticipated to be more flexible since it repels most liquid, from water to alkanes.⁸⁴⁻⁸⁵ Zhao et al. explain basic parameters of design for superoleophobicity and systematic research has initiated using the well-defined texture and geometry model pillar array surface.⁸⁶ Another part released information on the production processes.⁸⁶

Figure 8a shows the FOTS pillar surface SEM micrograph, consisting of $\sim 3 \mu\text{m}$ pillars of diameter $\sim 7.8 \mu\text{m}$ wide and $\sim 6 \mu\text{m}$ of pitch in height. SEM morphology with high magnification (insert) shows that each sidewall is composed of a wavy structural $\sim 300 \text{ nm}$, from top to bottom, which can be due to Bosch etching. Both static and dynamic methods of calculating contact angles, as well as the static contact angle with water and hexadecane are present in Figure 8b, have been studied as the surface property of FOTS pillar array surface.

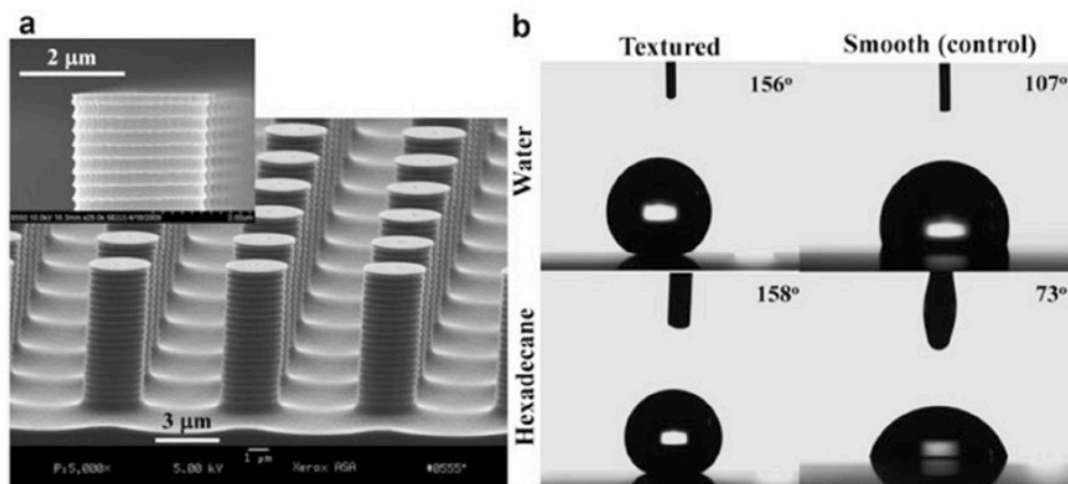


Figure 8: (a) SEM of FOTS on silicon-wafer (b) contact angle of static in water and FOTS on hexadecane (control smooth surface use FOTS on Si-wafer).⁸⁶

For the surface of the FOTS pillar series, the water and hexadecane touch angles are at 156° and 158° respectively and are substantially higher than for the 107° and 73° managed smooth surfaces. The findings indicate both surface texture and fluorination due to the high contact angles found for the surface pillar array FOTS. There is $\sim 10^\circ$ with both water and hexadecane of a sliding angle of the FOTS pillar size. The high contact angles and the low sliding angles lead to the conclusion that the surface of the FOTS pillar system is superhydrophobe as well as superoleophobe with low hysteresis.

The use of hydrophobe and photolithography to build micro / nano surfaces that are textured are not fresh.⁶⁹⁻⁷² The sidewalls of all the reporting pillars are smooth and only superhydrophobicity, not superoleophobicity, has been recorded. Tuteja and colleagues recently reported electrospun manufacture and superoleophobic mats that demonstrate.⁸⁷ The mat contains the nano fibres of poly-oligomeric F-POSS (1H,1H,2H,2H) and poly-methyl-methacrylate PMMA (pole(methyl) mixtures). With a hexadecane advance contact angle of $\sim 80^\circ$ the flat surfaces of the same substance are oleophilic. These authors have established the so-called silicon wafer micro hoodoo structure by photolithograph and surface fluorination in order to explain the mechanisms of the superoleophobicity of the electrospun mat. They concluded that re-entrant geometry is crucial to the achievement of superoleophobicity in the "micro-hoodoo" structure, and the ELM has a similar geometry on a liquid-solid-air composite interface. Further experimental and modelling experiments substantiate the finding.^{84-85, 88}

To sum up, we show that hydrocarbon oils would trap air pockets on rough surfaces with modular pillar arrays and result in a composite interface between Cassie and Baxter if the

following critical parameters were met: highly hexadecane angles of contact of the surface and a rough, overhang- or re-entrance-structured surface.

Biological advantage of superhydrophilic surfaces

An apparent benefit of regular irrigation is that plants do not suffer from any drought-induced stress in submerged water plants. Water on the surface thus limits the transfers of gas across the surface of the plant and can also create biofilms. Both impacts can reduce photosynthesis activity in plants.

For certain lower plants such as lichen, lichen and some mosses, which have no roots to suck up water and have no vascular system to hold water in other cases superhydrophilicity is the basis for storing water and nutrients. The water and nutrients in these animals are consumed fully surface regions. Superhydrophilic surfaces have also evolved for water and nutrient absorption in some higher plants, such as Bromeliaceae and epiphytic orchids.

In carnivorous plants, superhydrophilicity is used for capture and plant nutrition also works as well. It is not apparent if water spreads on surfaces of leaves that do not absorb nutrients. Water spread, e.g. on *Ruellia Devosiana* leaves, ensures that the water evaporates rapidly through an increase in the interaction between water and air. Water evaporates thus much more quickly from a super hydrophilic leaf than a superhydrophilic leaf, in which water forms semi-spherical or spherical droplets. This may serve as an effective strategy for reducing and growing microorganism growth in environments with regular rains, such as tropical rainforests. In *Ruellia devosiana*, water and molecules in the water will spread across the entire surface of the leaf in combination of structural roughness and secretion of hydrophilic components. The active components of the surface have still not been identified, but two observations are based on the assumption that *Ruellia* belongs to the Acanthaceae, a family of saponins. One statement was made by washing the leaves in water, popular for saponins, which results in the formation of foam. During the SEM investigations on leaves, another very important finding was made. Also mature leaves in a green house, grown for several months in a tropical setting, showed no signs of the development of biofilm on the leaves. The detergent property of saponins decreases water surface tension and is renowned for its antimicrobial and antifungal effects.⁸⁹ From these observations we suppose that saponins cause efficient water propagation and the water-saponin solution functions as an efficient self-protection mechanism against biofilm formation. This theory will however be demonstrated by further chemical analyses.

Literature review

Wettability with water

The water drop behaviour for numerous deciduous shrub and tree species from a temperate area was reported by Ewa et al.⁹⁰ The main goal of this research was to study leaf wettability variations in Polish forests (temperate climates) of 19 species (16 trees and 3 shrubs).⁹⁰ Parameters are collected as follows: 20 undamaged leaves have been selected for each plant and the wettability has been measured by contact angle measurements using the sessile drop method using an optical goniometer CAM 100.⁹⁰

Wang et al was investigated the wettability on surface of leaf in different type of plant (*Aloe vera*; *Hypericum monogynum*. *P. serrulata*; Ginkgo; and *Photinia serrulata*) by the analysis of surface morphology and contact angle.⁹¹ The microstructures of the Ginkgo leaf surface have long shapes and are aligned well, and are good for water diffusion.⁹¹ The research explores the effects of microstructures on surface weight, which illustrates surface design for various wettability requirements.⁹¹

He et al was reported the SFE of leaves of rice and rape with variations in leaf quality, the leaf and fluid surface, and the effect on the weight loss of drops, solid surface and PPP.⁹² They indicated that the SFE and wettability of crop-leaf surfaces should decide the acceptable PPP type and can be used as a valid guide to provide scientific guidance on how many factors affect the wettability of leaves and to enhance efficient use of PPP.⁹²

Fernández et al was reported the polarity, water absorption and wettability on leaves of Holm Oak.⁹³ The proof of water penetration through the upper leaf side was obtained in young and middle leaves 24 hours after drops had been deposited on the abax and adaxial surfaces.⁹³ Diverse microscopic and analytical techniques were used to analyse the structure and chemical composition of the abaxial (always present) and adaxial (only occurring with young leaves).⁹³

Bhardwaj et al was investigated the characteristic of wetting properties on surface of *Colocasia esculenta* leaf.⁹⁴ They studied the water repellence and the wetting properties of *Colocasia esculenta* (taro) and the engineered surface, which were bioinspired by the surface morphology of the leaf.⁹⁴ They calculated a steady, progressive and decreasing angle on the taroleaf, and the values for the lotus leaf are around 10 per cent lower.⁹⁴ They created bioinspired surfaces with hexagonal cavities of various size using standard techniques for photolithography.⁹⁴ The

ratio between the internal and the external radius of the circumcircle and the hexagon (b / a) was different.⁹⁴

Wettability with oil

Ramos et al was investigated the wettability and morphology on surface of leaf in the tree of Cashew from the Amazon, North Brazil.⁹⁵ It studied the effect on the hydrophobicity of *Anacardium occidentale* L. leaf surfaces of epicuticular wax grains.⁹⁵ Specimens of the leaf were examined directly with a metal-less microscope of an environmental electron scan. Static angle of contact between water and surface on both sides was also measured. An angle of $104.09^\circ \pm 0.95^\circ$ was found on the adaxial side, which indicates a hydrophobic surface adaxial surface. On the abaxial side, the angle of the epicuticular wax on the adaxial leaf surface was $62.20^\circ \pm 1.60^\circ$, which suggests hydrated existence. In this research, the plant of great medicinal and economic significance made an significant contribution towards the morphological and ultrastructural characterization of cashew tree leaves.⁹⁵

The wettability of pear leaves from three different climate areas after flowering was to be defined by Gao et al.⁹⁶ Leaves (greater SFE) became easier to wet, with a polar surface portion increasing overall, and age increased following blooms.⁹⁶ Changes in weather resistance have been predicted after flowering in various stages and regions in pear leaves ($P < 0.05$).⁹⁶

Kilwon Cho and his collaborators have identified the synthetic rice leaf-like wavy surfaces with anisotropic tunable wetting inspired by the hierarchical structures of the rice leaf surfaces.⁹⁷ The nanoscale rice leaf-like surfaces are managed to produce anisotropic and hydrophobic tunable properties that have transitioned between anisotropic / spinning / rolling, anisotropic and isotropic / rolling water droplet behaviour.⁹⁷ These remarkable changes are attributable to discontinuities on the contact line of the three-phase (solid-liquid-gas) due to the presence of air under the liquid regulated by the roughness of the nanostructures in the Hierarchy.⁹⁷

Sun et al was investigated the different wettability and mechanical analysis on Lotus leaf. In this analysis, the wetting of lotus leaves was compared to the hydrophobic mechanism of lotus leaves under four standard conditions, including fresh leaves. Weighting was determined for the various lotus leaves. Other experiments included measuring contact angle, the measurement of the microcosmic patterns of the lotus leaves by the electron microscope scan (SEM), a chemical analysis was made of wax extracted from the leaf surface.⁹⁸

Zhu et al was reported the wetting property on Oilseed Rapeseed. In this paper, the wetting of oilseed rapeseed with special surface structures is addressed for the first time. The fresh rapeseed flowers are super hydrophobic and display the self-cleaning properties similar to lotus leaves with a low adhesion force (AF). The fresh rapeseed leaves show hydrophobicity, in comparison, but high AF, resembling the petals of the rose. In addition, the effects of storage times on the wetting features of rapeseed leaves are studied. The hydrophobicity of the rapeseed leaves slowly becomes hydrophilic. In comparison, after putting at room temperature, the AF rises intensively for 10 days. This study provides a profound inspiration to develop high-hydrophobic biomimetic materials and various adhesion properties artificially.⁹⁹

The wettability analysis of the pesticides on rice leaf has been studied by Xu et al. The research aims to investigate the wettability in high-volume spray and spray atomizing concentrations in paddy fields of pesticide solutions. The wettability of most rice leaf pesticide solutions is low and therefore categories and surfactant contents in most pesticides must be changed. The rice leaf critical surface tension (CST) was calculated by the Zisman method and the national standard (GB 5549-90) was determined on the surface tension for 52 pesticides at concentrations of high volume and atomizing spray. It compares and analyses the relationship between CST and pesticide surface tension. The vital micelle concentration (CMC) of the surfactant in each pesticide was also determined by the surface tension changes of pesticide solutions and the wetting of the rice leaf solutions was demonstrated by 5 pesticides.¹⁰⁰

3. Conclusion

Several billion years of evolutionary cycles result in the variation of surface structures of the plant. Plants have established an extremely high surface diversity and versatility for their contact with the environment – Lotus' self-cleaning features are just one example. Millions of mutating and selecting years, testing and error: free knowledge for engineers and materials scientists.

The field Bionics is an old research & development field beginning around 1800, but for biomimetic applications surfaces had a relatively late function, the only exception being the 'Velcro fastener' of the 1950s. In the last two decades the publishing of the Lotus effect generated recognition among engineers and material scientists, words such as "superhydrophobicity."¹⁰¹ Surfaces play a rising role and it is expected that by 2019 the global nanocoatings market will hit US\$ 14.2 billion.¹⁰²

In the last three decades, biological surfaces have carried with them a large number of inventions. Surface technologies were influenced largely by bio-interface research and were based on technological advances relatively late. All the data show that the new age of bio-inspired surface technologies is just beginning.

It is important that we understand biomass surfaces — we have shown that this process is still under way. But the Anthropocene is also at the start of a significant loss of biodiversity. There are 10 million different species (possible models of biology) — in our evolving environment we lose a high degree of biodiversity and it has become evident to us that this also means the loss of the "living prototypes" for engineers, the biological role models.¹⁰³⁻¹⁰⁴ Bionics is just another attribute that should be viewed for the richness of life. The present and future use of superhydrophobicity includes reducing the formation and self-purification of biofilms. Superhydrophobic air retention surfaces can also be a clever solution to improving the power-saving surfaces of pipes or boats during water movement. Superhydrophilicity in plants is not only dependent on smooth surfaces in submarine plants, but is also due to the structure of the surface such as water absorbing fur, porous and spongelike structures and raw convex surfaces. Water and nutrient absorption and rapid water evaporation from the surfaces are the biological benefits of such weighing phenomena. Superhydrophilicity is beneficial in preventing droplet formation by condensing on surfaces and offers an intelligent strategy to prevent glass, window, reflection and other surfaces. For energy-efficient liquid transport on micro and capillary systems, the use of capillary transport through superhydrophobic surfaces will in future be used.

4. Corresponding author

Corresponding author

*Email: xxxx@gmail.com (Dr. XXX)

ORCID

Name 1: 0000-xxxx-xxxx-xxxx

Name 2: 0000-xxxx-xxxx-xxxx

Name 3: 0000-xxxx-xxxx-xxxx

5. Author Contributions

All the experiments and application were performed by XXXX, XXX and XXX under supervision of XXXX and XXX. The manuscript was written by XXX and reviewed by XXX and XXXX.